

SCIENTIFIC REPORTS



OPEN

Analyzing historical land use changes using a Historical Land Use Reconstruction Model: a case study in Zhenlai County, northeastern China

Received: 29 September 2016

Accepted: 14 December 2016

Published: 30 January 2017

Yuanyuan Yang^{1,2}, Shuwen Zhang³, Yansui Liu^{1,2}, Xiaoshi Xing⁴ & Alex de Sherbinin⁴

Historical land use information is essential to understanding the impact of anthropogenic modification of land use/cover on the temporal dynamics of environmental and ecological issues. However, due to a lack of spatial explicitness, complete thematic details and the conversion types for historical land use changes, the majority of historical land use reconstructions do not sufficiently meet the requirements for an adequate model. Considering these shortcomings, we explored the possibility of constructing a spatially-explicit modeling framework (HLURM: Historical Land Use Reconstruction Model). Then a three-map comparison method was adopted to validate the projected reconstruction map. The reconstruction suggested that the HLURM model performed well in the spatial reconstruction of various land-use categories, and had a higher figure of merit (48.19%) than models used in other case studies. The largest land use/cover type in the study area was determined to be grassland, followed by arable land and wetland. Using the three-map comparison, we noticed that the major discrepancies in land use changes among the three maps were as a result of inconsistencies in the classification of land-use categories during the study period, rather than as a result of the simulation model.

Decadal-centennial land use and land cover change (LUCC) has been considered as a vital driver of global environmental change^{1–5}. Historical land use information is essential in understanding how anthropogenic land use and land cover change has influenced the temporal dynamics of environmental and ecological issues, including soil degradation^{6,7}, water quality^{8,9}, habitat loss and fragmentation¹⁰, biodiversity loss^{11,12}, climate change^{13–15} and, most importantly, the global carbon balance¹⁶. However, a primary obstacle in assessing the consequences of land use changes is the lack of high-resolution, spatially explicit and thematically complete historical land-use change data, as well as the conversion types that feed into the models related to the above ecological issues⁷.

Due to a lack of available adequate historical datasets, the reconstruction of historical land use/cover relies on existing databases containing local/regional level statistics or records, population statistics, historical maps and model assumptions⁵. Recently, substantial progress has been made in gathering historical land use data and producing historical reconstructions, with an increase in investigations at both the global and regional scales^{17–32}. The changes have been discussed in detail through a review of historical reconstruction methods of LUCC³³. The majority of current studies fail to thematically represent the land area in its entirety, and also fail to include competing land-use categories and land conversion types⁵. For example, present researches target arable land, wetland and forestland, but do not provide information regarding land-use categories such as settlements, water bodies or other land use types.

Model-based reconstructions of land-use change are rapidly advancing as anthropogenic land-use change is one of the most important drivers of environmental change. As the accumulation of human activities' impact on

¹Institute of Geographic Sciences and Natural Resources, Chinese Academy of Sciences, Beijing 100101, China.

²College of Resources Science and Technology, Beijing Normal University, Beijing 100875, China. ³Northeast Institute of Geography and Agroecology, Chinese Academy Sciences, Changchun 130102, China. ⁴Center for International Earth Science Information Network (CIESIN), Earth Institute, Columbia University, Palisades, NY 10964, USA. Correspondence and requests for materials should be addressed to Y.Y. (email: sophiayangyuanyuan@hotmail.com)

the earth's surface, present land use pattern contains the essential information about historical land use patterns. Meanwhile, remote-sensing technique makes it feasible and convenient to observe the global characterization of land use/cover with high resolution and thus the present land-use spatial pattern is the most crucial information for historical land reconstruction. In general, the spatial allocation method is under the assumption of similarities between historical land use spatial patterns and present spatial patterns. Related models have been divided into three types according to the various effects on controlling the similarities: totally dependent, partially dependent and dynamically dependent³⁴. The differences among the three types lie in the different spatial allocation principles. The totally dependent approach means that historical land-use pattern is completely decided by the present one in the reconstruction model. That is, the proportion of the allocated area (amount) in each grid accounting for the total area (amount) in an administrative area (country or province) is an invariable in spatial allocation by adopting downscaling or other ways. The partially dependent approach is to avoid “using today's pattern for historical reference” and it focuses on the driving mechanism research of spatial pattern. Generally, the partially dependent approach is based on an assumption that the range of historical agricultural activities could not exceed the present one. The dynamically dependent approach has the sophisticated algorithms and takes the effect of time into consideration³⁴, initially proposed by Goldewijk³⁵ in his HYDE 3.1 (History Database of the Global Environment) application³⁵. The driving force of land use process has to be clarified and the land-use change trajectories have to be analyzed before using the partially dependent approach. After this, a land use forecasting model (e.g., cellular automata, Geomod) as a carrier can be used to produce a backward simulation. In this context, to enhance our understanding of the degree and extent of global and regional anthropogenic changes in land use patterns^{36,37}, a spatial-explicit modeling framework (HLURM: Historical Land Use Reconstruction Model) is explored and proposed in this paper. Currently, there is a growing demand for harmonized, spatially explicit and high resolution land-use change products. Our model will aim to satisfy this demand. This model approach can also produce backward projections by analyzing land use changes over time, and it is a dynamically dependent approach based on the assumption that current spatial land use pattern is intrinsically linked to historical patterns.

As the third largest and most populated country, China has a long history of agricultural civilization and its land use has undergone great changes owing to significant transformation caused by human activities, natural factors and their impact on the climate and environment^{38,39}, which plays a significant role in the global LUCC pattern⁴⁰. Over the last century, northeastern China has experienced large-scale population reflux of Chuang Guandong migration and major land reclamation process influenced by lifting the ban on the Qing Government's prohibition policy^{41–43}. As a result, it is one of the regions in China witnessing dramatic LUCC in a century time scale⁴¹. Here, considering the richness of historical documents and the availability of regional LUCC data derived from the historical topographic maps, physical environmental background maps including those of terrain, climate, geology, soil, vegetation and hydrology as well as socioeconomic statistical data based on our previous research, we choose to represent Zhenlai County, located in northwestern Jilin province, as a case study. As a part of farming-pastoral ecotone of northern China, the eco-environment in Zhenlai County is very fragile and is liable to the disturbance of various factors⁴¹. In this research, we try to explore a spatial-explicit modeling framework (HLURM) by using the dynamically dependent spatial-allocation approach and then apply this modeling framework to the historical reconstruction of spatial distribution of land use/cover in the early reclaimed time of northeastern China to check its modeling behavior. The overall objectives of this paper are: (1) to reconstruct historical land use during the early period of reclamation (1930s) in Zhenlai County using a 90 m × 90 m HLURM model to generate a backward projection; and (2) to validate the results of the reconstruction by means of a three-map comparison, assessing its accuracy by classifying pixels into the following four types: null successes, hits, misses and false alarms. This research will make us understand better the historical land use and land cover change over the past century in northeastern China and provide harmonized, spatially explicit and high resolution land use change products to ecological issues' study.

Materials and Methods

Study Area. Zhenlai County (N45°28'–N46°18', E122°47'–E124°04'; Fig. 1) is a typical part of the farming-pastoral ecotone of northern China. Under the governance of Baicheng city, Zhenlai County lies in the northernmost part of Jilin province, and it borders Heilongjiang to the east and Inner Mongolia to the west. Historically, the region comprised nomadic land for Mongol princes, and it was only after the enactment of a policy lifting the ban on land reclamation during the late Qing dynasty (1902) that inhabitants were able to reclaim land. In 1910, the county was established as Zhendong County and was later merged with Laibei County in 1947, and this combined region was later renamed Zhenlai County. The region has experienced dramatic LUCC over the past century, and the land reclamation process is relatively complete. The county is rich in geomorphologic features with high elevation in the northwest and low elevation in the southeast. The northwestern area is adjacent to the Greater Hinggan Range and the central areas mostly comprise rolling hilly land. The eastern and southern regions surround the Nenjiang and Tao'er Rivers, respectively, forming a fertile flood plain on both riverbanks. The main soil types include chernozem, alluvium soil, alkali soil and meadow soil. As this region is located in the inland mid-latitude areas, it comprises a temperate, continental monsoon climate with distinct seasonality. Mean annual rainfall is 402.4mm and is unevenly distributed across time. Mean annual evaporation is 1755.9 mm, which is approximately four times greater than the mean annual rainfall. This low volume of precipitation and high level of evaporation results in a drought-prone climate in the area, especially in the spring. The mean annual temperature is approximately 4.9 °C.

Data. One Landsat MSS (Multispectral Scanner) and two Landsat TM (Thematic Mapper) images were selected for the years 1976, 2000 and 2005. These remote sensing images were used to interpret and vectorize land use data obtained from the United States Geological Survey (USGS; <http://glovis.usgs.gov/>). A series of

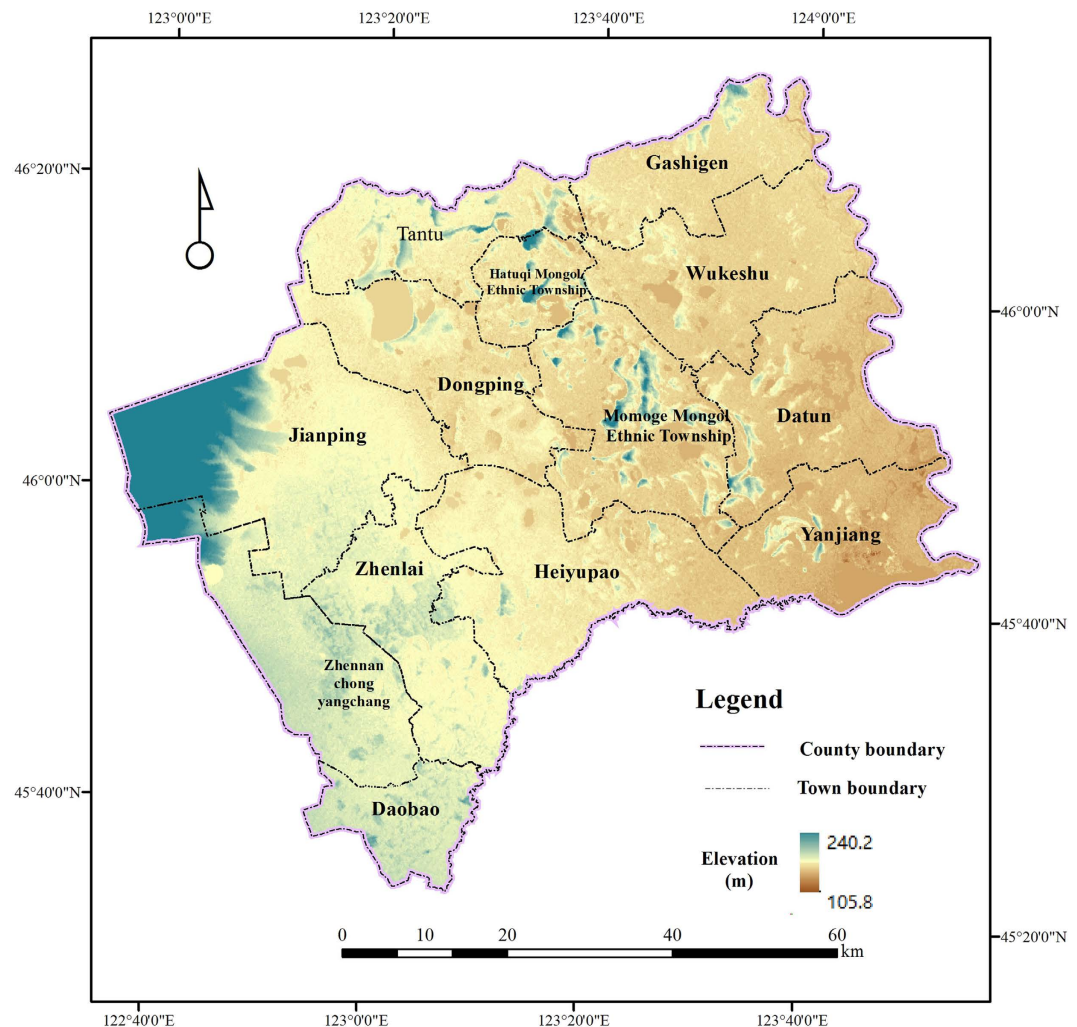


Figure 1. Map of the study area, Zhenlai County (map created using ARCGIS 10).

topographic maps from the 1930s (in the year of 1932 drawn to scale at 1:50 000, in the year of 1935 at 1:100 000 and 1:500 000, respectively) were also collected and digitized. The historical spatiotemporal distribution of land use and land cover in 1954 was also reconstructed by consulting and incorporating information relating to terrain, climate, geology, soil, vegetation, hydrology and socioeconomic statistical data from topographic maps and physical environmental background maps^{44,45}. Soil data was digitized from the “*Local Record of Zhenlai County*”. A slope raster was generated using a 90 m raster DEM obtained from the Shuttle Radar Topography Mission (SRTM).

Classification system. As land use types indicated on the topographic maps and remote sensing images used in this study differed, we initially produced a map series with unified contents. In order to make temporal comparisons, the maps also had to be thematically generalized. Considering both the local characteristics as well as the predominant land use classification system used in China⁴⁶, the available land classes were aggregated into seven suitable land-use categories for this study: arable land, forestland, grassland, water, settlement (urban and rural construction), wetland and other unused land (including sand, saline-alkali soils and bare land)^{47,48}.

HLURM model. The Historical Land Use Reconstruction Model (HLURM) provides a high-resolution reconstruction of historical land use spatial distributions. The model outputs are based on the assumption that the present spatial pattern of land use is intrinsically dependent on a historical pattern.

HLURM theory. Considering the natural, social and economic predictors of changes in land use and land cover, HLURM takes into account regional land use changes since the advent of remote sensing. This was undertaken by taking the grid as the research unit, calculating the probability of each land type in each grid to determine the most likely land-use category and then using the land type with the largest probability to reveal the land use in the research units. A cellular automata (CA) model was then used to produce a backward simulation as a carrier.

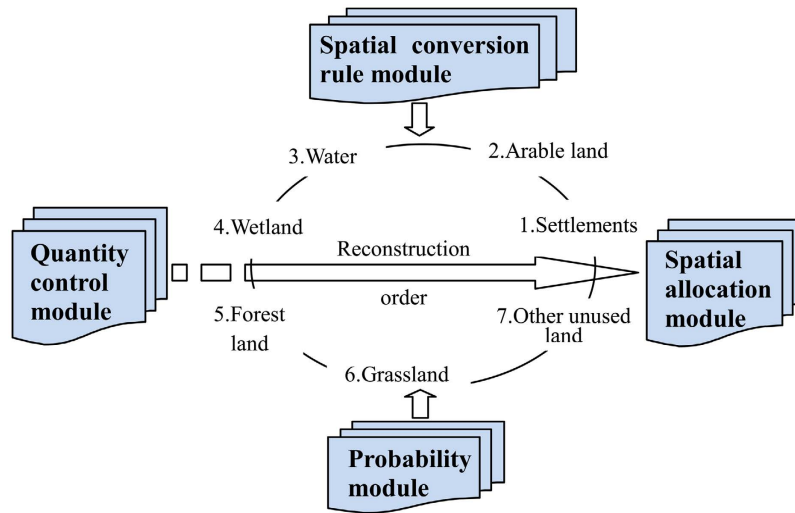


Figure 2. HLURM's four modules.

HLURM modeling framework. The HLURM model consists of four main modules: quantity control module (QM), spatial conversion rule module (CM), probability module (PM) and spatial allocation module (AM) (Fig. 2).

Quantity control module (QM), also known as the demand-constraint module, is the basis of HLURM model and also the premise of the spatial reconstruction. This module can be operated and run independently of the HLURM model. In general, total quantity of land use can be determined in two ways: (a) collecting historical documents and calibrating the available data; and (b) modeling quantitatively from the simple historical trend extrapolation method to the relatively complicated economic model. Appropriate model of backward projection for land use quantity should be chosen according to the actual circumstance.

Spatial conversion rule module (CM) establishes historical rules for land use and land cover change. This module contains analysis of both land use conversion sensitivity and land use conversion sequence. Land use conversion sensitivity monitors the conversion characteristics and trends among land-use categories during each time interval; obtains the transformation probabilities for land dynamics in the study period; and clarifies the trajectories of land use changes. These factors provide fundamental basis for analyzing the land use conversion sequence. CM will then reveal land dynamic characteristics and provide essential data for the following probability module, as well as producing the constraints for the spatial allocation module.

Probability module (PM) calculates the probability of each land type in each grid based on probability theory. By analyzing the relationships between both various natural environmental conditions and socio-economic conditions and land-use distributions, a land suitability evaluation map is produced to exhibit the possible spatial distribution of historical land cover. According to current research about land use and land cover change, three assumptions of HLURM are proposed to operate the PM module: 1) The current spatial land use pattern is intrinsically dependent on a historical pattern; 2) The boundary of historical land use with human activities, such as arable land and settlements, does not exceed the union range of each land use type in the study period; 3) The natural environmental factors of land suitability have not changed over time during the past century due to the limitation of data collection.

Spatial allocation module (AM) distributes the quantity of each land use into the geographical locations and spatially explicit outcomes according to certain principles or approaches. It then realizes the backward projection of historical land use. For specific spatial allocation, downscaling can be used in the descending order of distribution probability under the control of total land-cover area and other distribution factors.

According to the influence of human activities on land use and the characteristics of land use, the reconstruction order for land-use categories in this study is as follows: settlements, arable land, water, wetland, forestland, grassland and other unused land. Different spatial constraints are established for land-use categories and then spatial grid allocation is operated under these constrains.

Three-map comparison. The maps used for the three-map validation of the LUCC model included reference time 1, reference time 2 and simulation time 2. Comparisons between the maps of reference time 1 and reference time 2 characterized the observed changes in the maps, reflecting the dynamics of the land use. Comparisons between the maps of reference time 1 and simulated time 2 characterized the predicted changes, demonstrating the model behavior. Model validation estimates the agreement (or error) stemming from the comparison between the maps of simulation time 2 and the reference (or real) time 2. Here, the model accuracy was assessed by determining the four components of accuracy and error, namely, null successes (accuracy of observed versus predicted persistence), hits (accuracy of observed versus predicted change) misses (error due to observed change predicted as persistence) and false alarms (error due to observed persistence predicted as change). The summary statistics for error due to quantity (EQ, Eq. 4) and error due to allocation (EA, Eq. 5) were also assessed^{49,50}. Quantity error reflects the inability of the model to perfectly predict the quantity of net change, and is not influenced by spatial

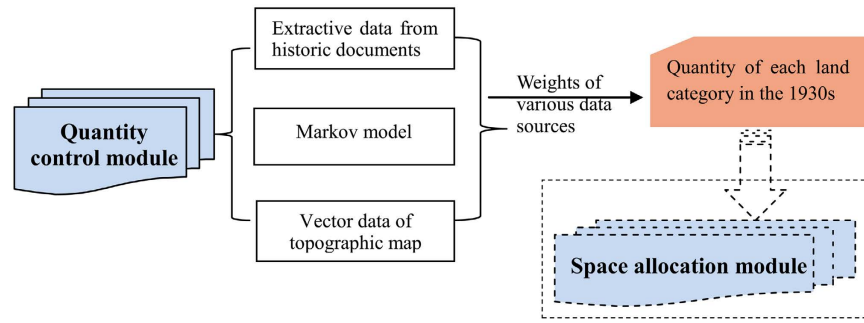


Figure 3. Quantity control module.

allocation. Conversely, allocation error is associated with the inadequate ability of the model to allocate pixels of change across the landscape. This error derives from the spatial allocation algorithm, which is associated with the independent variables in the model. The error might be sensitive to any modification of the spatial allocation algorithm. In addition, the figure of merit (FOM, Eq. 6) and the three ratio indices (Eqs 7–9) that quantify the amount of hits, misses and false alarms relative to the observed change, were also determined. The FOM is calculated by dividing the hits by the sum of hits, misses and false alarms and, in the case of the models that simulate several categories, removing the partial hits from the numerator. This measure allows a more realistic assessment of the cell-to-cell coincidence between simulated and real maps than more commonly used metrics, such as the kappa index or overall accuracy, which are usually calculated using the entire surface area⁵¹. The FOM ranges from 0% (no overlap between observed and predicted change) to 100% (perfect overlap between observed and predicted change)⁵².

$$OC \equiv \text{Observed Change} = M + H \quad (1)$$

$$PC \equiv \text{Predicted Change} = H + F \quad (2)$$

$$T \equiv \text{Total Error} = M + F \quad (3)$$

$$EQ = |PC - OC| = |(H + F) - (M + H)| = |F - M| \quad (4)$$

$$EA = T - Q = (M + F) - |F - M| = 2 \times \text{Minimum}(F, M) \quad (5)$$

$$FOM = \frac{H}{H + M + F} \times 100 \quad (6)$$

$$HOC = \frac{H}{H + M} \quad (7)$$

$$MOC = \frac{M}{H + M} \quad (8)$$

$$FOC = \frac{F}{H + M} \quad (9)$$

where, H, M and F are the hits, misses and false alarms; HOC, MOC and FOC are, respectively, the ratio of hits, misses and false alarms to the observed change, which is the summation of the hits and misses.

Results

Quantity control module. Based on available historical data, the total quantity of each land use was calculated according to the weights of various data sources, such as historical documents, Markov model results and vector data derived from topographic maps (Fig. 3).

The spatiotemporal Markov Chain model uses transitional probabilities to model change over time among land-use categories, and is able to simulate several land-use categories simultaneously. However, due to temporal changes in the various land-use categories, transition matrices describing various types of land cover from $t - 1$ to t might not be totally consistent with those in the period between t and $t + 1$. Thus, the transition matrices were modified by analyzing land use changes over the last few decades, and were also used to define the rules for AM, assuming that current spatial pattern of land use is inherently dependent on the historical pattern. In this context, in order to account for the period between 1932 and 1954, transition matrices were revised between 1954 and

Land-use categories		Modified data of Markov results	Extractive data from historical documents	Data derived from the topographic maps (DTM)			Weighted area
				i	ii	iii	
Arable land	Area (ha)	146598.14	85938.43	204012.98	143744.76	99902.81	129966.07
	Weight	0.293	0.178	0.089	0.219	0.221	
Forestland	Area (ha)	630.5	—	555.48	881.96	438.98	675.69
	Weight	0.308	—	0.073	0.382	0.237	
Grassland	Area (ha)	221456.34	—	270651.67	346339.5	409115.25	335798.79
	Weight	0.217	—	0.074	0.356	0.353	
Water	Area (ha)	11888.5	—	7755.28	6759.83	6149.02	9274.14
	Weight	0.485	—	0.116	0.254	0.145	
Settlement	Area (ha)	1801.49	—	—	2383.36	5613.1	3758.57
	Weight	0.151	—	—	0.396	0.453	
Wetland	Area (ha)	148313.62	—	48630.73	31496.73	10386.98	51514.18
	Weight	0.202	—	0.157	0.344	0.297	
Other unused land	Area (ha)	916.85	Correction under the control of total area				618.69

Table 1. Areas and weights of various land use types in the 1930 s. Note: DTMi - data derived from the topographic maps at scale 1:500,000 in the 1930 s; DTMii - data derived from the topographic maps at scale 1:100,000 in the 1930 s; DTMiii - data derived from the topographic maps at scale 1:50,000 in the 1930 s.

1976 according to the rules governing LUCC in the study area from 1954 to 2005. The analysis of land use changes indicated that nearby forests and wetlands would not be utilized until all of the grassland suitable for farming was reclaimed⁴⁷. Hence, we added the grid numbers for wetland converted into arable land from 1954 to 1976 to grassland. In addition, climate change, especially precipitation, had a significant impact on wetlands due to the smooth landscape in the study area. Gao⁵³ indicated that northeast China experienced a drier period between 1900–1935, a wetter period between 1936–1959 and another dry period after 1960. In light of this we adjusted the area of “wetland → water” into the area of “wetland → grassland” from 1954–1932. Finally, the area of each land use was obtained by modifying Markov results.

Weight is often used to develop a set of relative weights for a group of factors in a multi-criteria evaluation. Here, the analytic hierarchy process (AHP) approach, calculating from “WEIGHT-AHP weight derivation” module of the IDRISI Selva software, was used to determine the weights of land-use categories from different data sources in the 1930 s based on the area of various land use from multi-source data and the reaction characteristics of land-use categories in these different data sources. Under the control of 531606.14 ha of the total study area, the areas of land-use categories in the 1930 s were obtained. Table 1 shows that grassland dominated the largest area of land cover (334798.79 ha) with arable land (129966.07 ha) being the second most dominant. The areas of forest land, water, settlement, wetland and other unused land were 675.69 ha, 9274.14 ha, 3758.57 ha, 51514.18 ha and 618.69 ha, respectively.

Spatial conversion rule module. Research regarding the spatial conversion rule module was comprehensively explained and discussed in the spatiotemporal changes’ analysis from 1954 to 2005 in the study area^{47,48}. Results from our analysis (Fig. 4) enable the following conclusions to be made according to spatial conversion rules for various land use: (1) Arable land expanded at the expense of grassland and wetland. At the same time, a large proportion of grassland was converted into unused land, reflecting the remarkable environmental degradation experienced in Zhenlai County during the study period. (2) Trajectory analysis of land use and land cover change demonstrated that settlements, arable land and water bodies remained relatively stable in terms of coverage and spatial distribution, while grassland, wetland and forestland demonstrated weak stability. (3) While natural processes dominated environmental change in the study area, anthropogenic influences also played an important role. (4) The Lorenz curve/Gini coefficient indicated that arable land was the most scattered, whereas forestland was the most concentrated.

Probability module. Factors and constraints were the two types of criteria used in this study (Fig. 5); a factor signified a continuous degree of fuzzy membership (in the range of 0 ± 255), while constraints limited the alternatives altogether (i.e. fuzzy membership is either 0 or 1)⁵⁴. The factors for suitability maps included the following three kinds: environmental influential factors (geomorphology data, topographic data such as slope, aspect and elevation, soil data, Fig. 6a); human disturbance factors (distance from settlements, rivers and roads, Fig. 6b); and autocorrelation factors (Fig. 6c). Each grid cell in all of the digital raster maps represented an area of $90\text{ m} \times 90\text{ m}$, which is considered an accurate representation of the land-cover in the study area. Such precision avoids losing the resolution of the data, though it could result in data redundancy. Aiming to union each land-use category by overlaying land use maps in several time points, this module calculated the percentage of each land-use category distributed in these five natural factors to represent the probability of each land use in each grid under different environment backgrounds by intersecting the above union (\cup) dataset with various environment background data. We also digitized settlements, rivers and road layers from the 1930 s topographic maps, calculated their Euclidean distances and then dispersed the distance value within the range of 0–1; where 0 represented the

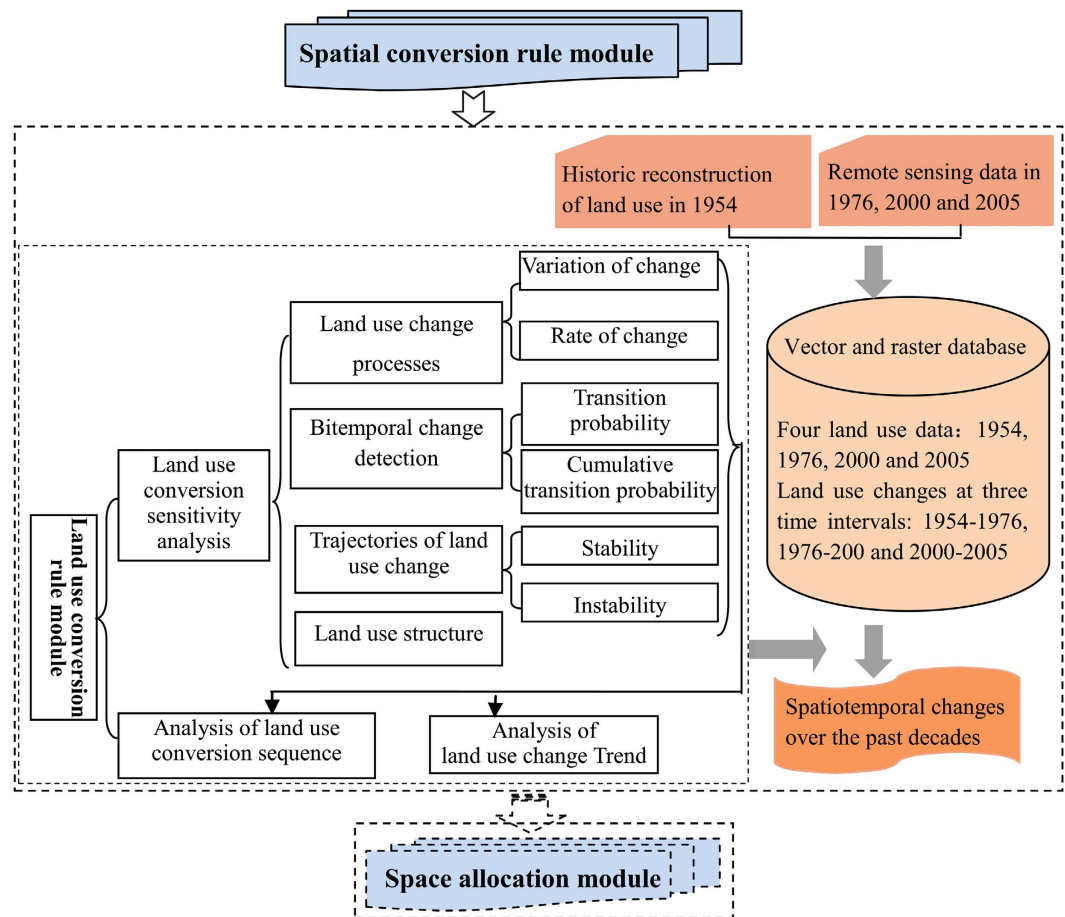


Figure 4. Spatial conversion rule module.

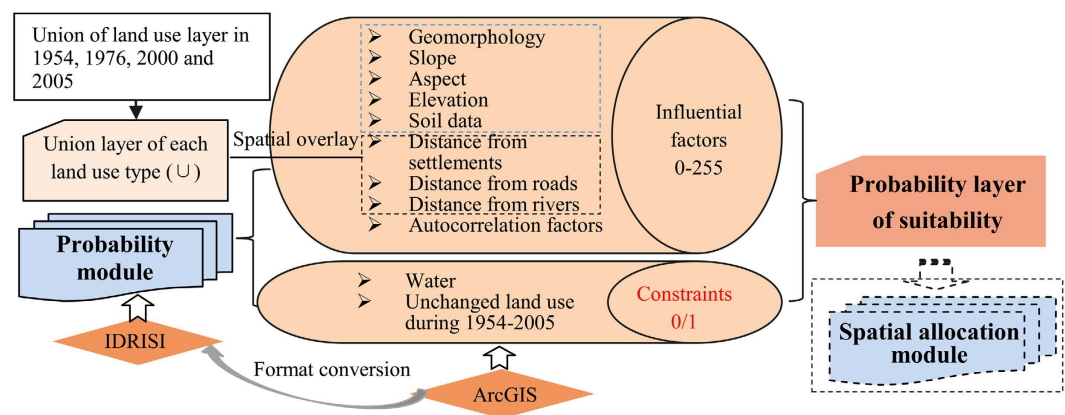


Figure 5. Probability module.

nearest distance and 1 represented the farthest distance. In addition, in accordance with the principle of spatial autocorrelation that suggests that certain land use types favor a certain land cover⁵⁵, we also used the spatial autocorrelation distance of each land-use category based on 1954 land use map. Finally, the hundred-mark system about the percentage of each land-use category in the five natural factors was converted into a 255-mark system while the distance values with the range of 0–1 about human disturbance factors and autocorrelation factors were reverse-extended to 255–0. These were then calculated by standard formula for grid computing to meet the demand of this module.

Here, two constraints were considered: water and unchanged land-cover during 1954 and 2005. Based on the previous three assumptions of the PM, we concluded that the unchanged land use from 1954–2005 had existed in 1932. Considering that the other six land cover types do not typically occur on bodies of water, water layers

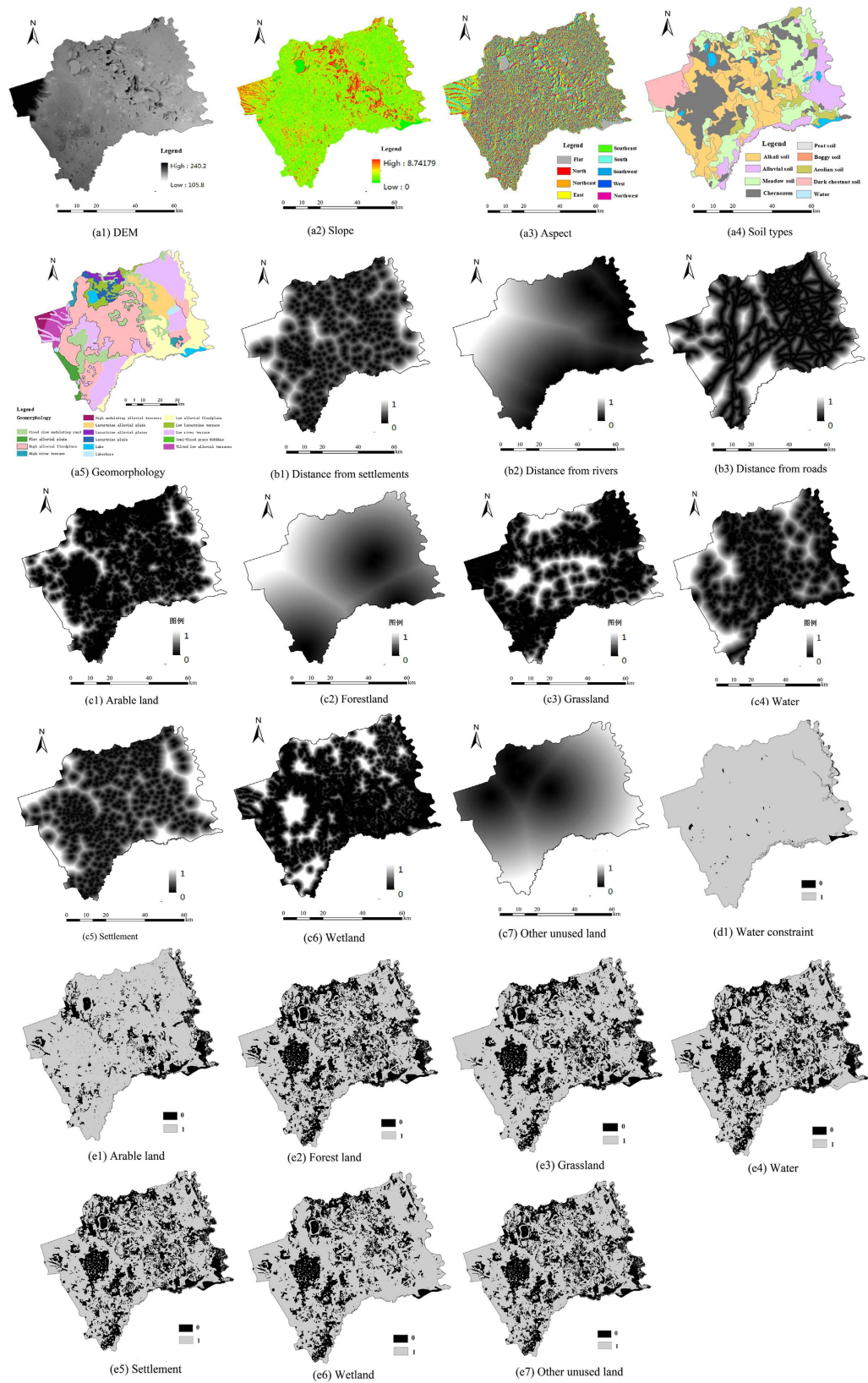


Figure 6. Environmental influential factors for suitability maps (a1–a5); human disturbance factors (b1–b3); spatial autocorrelation distance factors (c1–c7); and constraint images for water (d1) and unchanged land cover (e1–e7) (map created using ARCGIS 10).

Factors		Arable land	Forestland	Grassland	Water	Settlements	Wetland	Other unused land
Environmental influential factors	Soil	0.232	0.127	0.058	0.294	0.032	0.085	0.021
	Geomorphology	0.054	0.027	0.051	0.209	0.012	0.021	0.063
	Elevation	0.032	0.031	0.031	0.103	0.038	0.143	0.004
	Slope	0.036	0.025	0.071	0.098	0.059	0.111	0.006
human disturbance factors	Aspect	0.005	0.012	0.033	0.071	0.005	0.107	0.009
	Distance from river	0.096		0.099		0.101		
	Distance from roads	0.092	0.072			0.124		
	Distance from settlement	0.213	0.369			0.309		
Spatial auto-correlation factors	Arable land	0.24						
	Forestland		0.337					
	Grassland			0.304			0.162	0.124
	Water				0.225			
	Settlement					0.32		
	Wetland			0.189			0.296	0.205
	Other unused land			0.164			0.075	0.568

Table 2. Factors and their weights used in the construction of suitability maps.

digitized from the 1930s topographic maps (Fig. 6d1) were subjected to the same constraints as all the other land use/cover types, excepting themselves. In terms of long-term landscape development, the degree of unchanged land use across the study period was relatively stable and consistent in its spatial distribution. We thus made the assumption that the degree of unchanged land cover over the past 60 years had also existed in the 1930s, and the present land use pattern is dependent upon the historical one. Thus, a particular land use type could not develop where a different land cover had existed at that time (Fig. 6e).

We made use of the MCE process involving criteria of varying importance in accordance with decision makers along with information regarding the relative importance of the criteria. It is generally obtained by assigning a weight to each factor. The weights given to different factors in this study were generated using Saaty's Analytical Hierarchy Process (AHP), where a larger weight denotes a more important criterion in terms of overall utility (Table 2). The probability module was completed using IDRISI Selva software and the suitability maps for various land-use categories are shown in Fig. 7.

Spatial allocation module. This module, based on the algorithm of the cellular automata (CA) model, has two kinds of spatial constraints: (1) interpretation results of topographic maps; and (2) the spatial probability of each land-use category. The specific spatial allocation process is shown in Fig. 8. There were a number of procedures in this module: (1) whether or not the probability of land use is the largest in the land suitability probability layer; (2) whether or not it is consistent with the data derived from the topographic maps; (3) checking neighbor status to judge whether or not the number of one land-use category around the neighbor grids is equal to or greater than five; (4) whether or not this certain land use type reaches the upper limit of its total quantity. If the land use type has reached its upper limit then the procedure ends; otherwise, the procedure returns to the above process to continue to judge; (5) the reconstruction order for land-use categories is as follows in the process of spatial allocation: settlements, arable land, water, wetland, forestland, grassland and other unused land.

The spatial allocation module is programmed in Matlab software and the 1930s land-use map simulated by the HLURM model could be output by spatial allocation module (Fig. 9). It can be seen that grassland dominated land cover (63.17%), a result which was expected given the large number of immigrants that settled in this area, resulting in the reclamation of wildland and grassland. Anthropogenic activities intensified following the enactment of the policy lifting the ban on land reclamation in northeastern China in the late Qing Dynasty. Arable land accounted for the second largest land cover (24.45%), the majority of this land type being located in the flat areas of the central and western parts, as well as in the north. The arable land was also found to be scattered between the other areas. The wetland accounted for 9.69% of the total area and it was mainly distributing to the east and south along the Nenjiang River and the Tao'er River. The area of water bodies consisted of 1.74% of land cover while the area proportions of settlements, forestland and other unused land were 0.71%, 0.13% and 0.12%, respectively.

Discussion

Through producing a backward projection, the HLURM model creates a high-resolution historical reconstruction of land use and land cover in Zhenlai County in the 1930s. A common method to test the reliability of historical reconstructions involves comparing with information from a variety of independent sources⁵⁶. Detailed historical maps are valuable sources for land cover reconstruction as these can be used to directly digitize historical land cover. We compared the contemporary HLURM model results with historical 1:100,000 topographic maps as these allowed us to analyze land use on a regional scale⁵⁷. According to a three-map comparison, we were able to validate the model by identifying all potential prediction successes and errors. The three maps included the observed 1954 land-use map, the observed 1932 land-use map digitized from the topographic maps and the predicted 1932 land-use map. As six land-use categories were present in the digitized topographic maps, we decided to combine wetlands and other unused land types into unused land in both the reference 1954 map and simulated

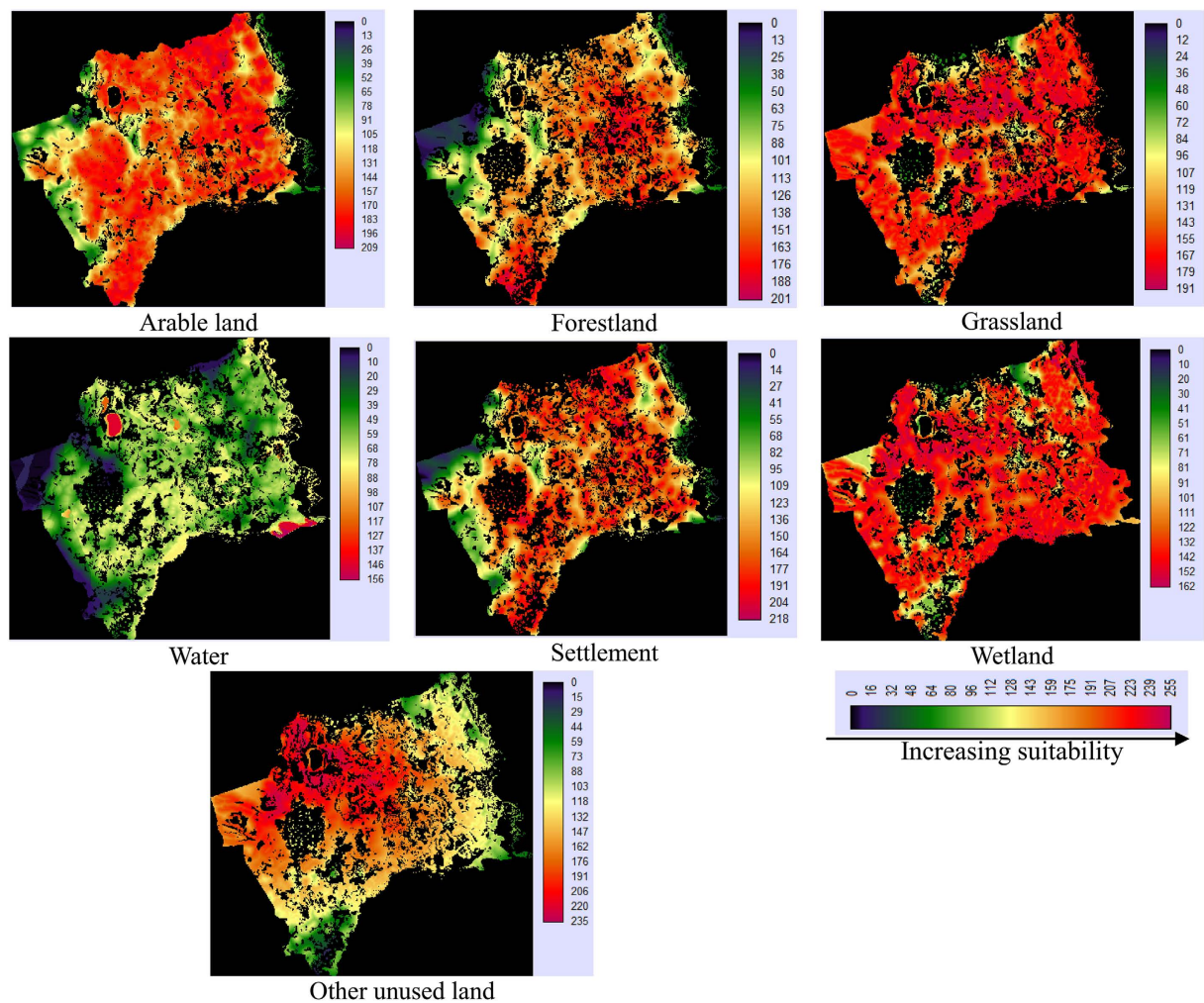


Figure 7. Suitability maps for various land-use categories (map created using IDRISI Selva).

1932 map. Thus, six land categories were defined for comparison: arable land, forestland, grassland, water bodies, settlements and unused land.

Figure 10a indicates the percentage of area covered by each land-use category in the reference 1954, reference 1932 and simulated 1932 maps. The largest categories, as indicated by the pie charts, were grassland, arable land and unused land. While the pie charts provide useful information regarding the contribution of each land category, they fail to provide much detail concerning individual transitions among categories. Thus, we overlaid the reference 1954 and 1932 maps, and the reference 1954 and simulated 1932 maps, in order to analyze the changes between 1954 and 1932. Two matrices were produced and are presented in Table 3, and the contribution of each category at the initial time (1954) and at the final time (1932) are indicated. Figure 11b,c and Table 3 illustrate the gross losses and gains in land use types, the majority of which were concentrated in the central parts of the study area as well as in the vicinity of rivers and lakes. The total area change for the reference map was 306,161.00 ha while it was only 195,500.47 ha for the simulated map. Notably, a substantial amount of land classified as unused in 1954 was marked as grassland in 1932 in both the maps, especially the reference map. The spatial location of settlements over time was difficult to reconstruct due to their negligible size compared to the other land-use types, as well as the high temporal variability and plasticity in site preferences⁵⁸. Furthermore, as this research focused on natural factors and excluded other potential drivers (e.g. cultural and socioeconomic driving forces), the reconstruction of settlement areas was unsatisfactory as several differences regarding gross gains and losses existed between the reference and the simulated change maps.

The comparison of observed and predicted change is shown in Fig. 11 where four types of accuracy and error were distinguished. This map was created using an overlay of the predicted land use map of 1932 and the reference map of 1954 in order to reflect landscape persistence versus change. Over the entire study area, the simulated 1932 land use map reported 36.45% null successes, 30.62% hits, 26.97% misses and 5.95% false alarms. Observed change (OC) occurred on 57.59% of the land use, whereas the predicted change (PC) occurred on 36.58% of the land use. Overall, there was a total EQ (error due to quantity) of 21.02%, an EA (error due to allocation) of 11.91% and a total error of 32.93%. This indicates that a minor allocation disagreement and a major quality disagreement existed. The total error is smaller than the observed change, suggesting that this model is more accurate than a

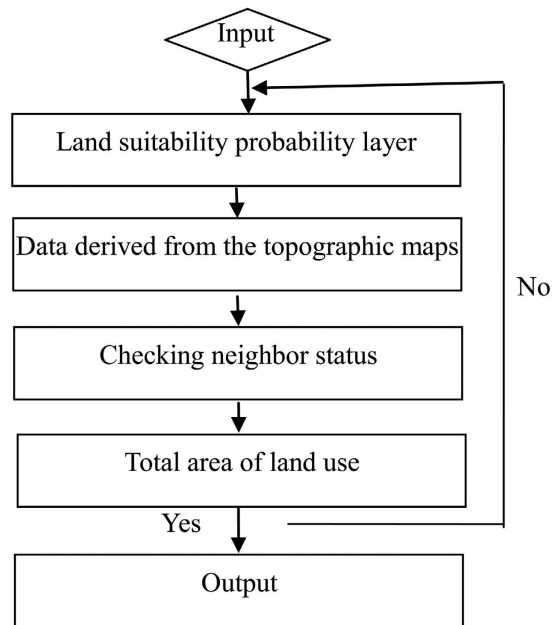


Figure 8. Flow chart of spatial allocation module.

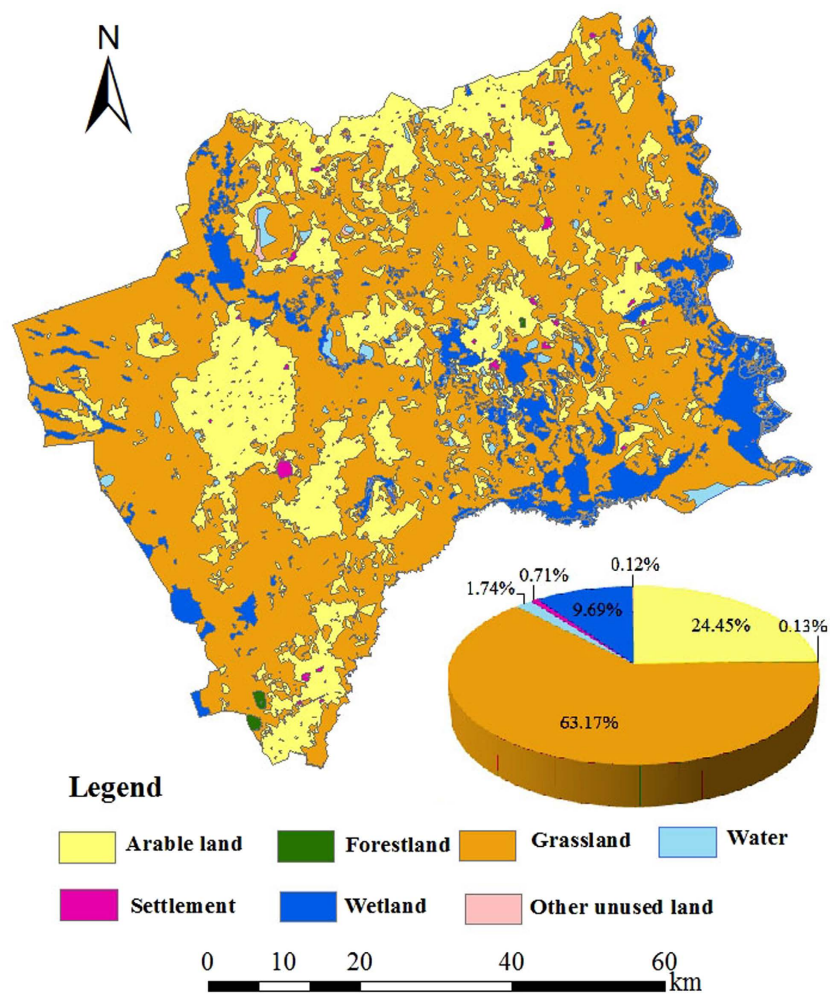


Figure 9. HLURM simulation of land-use map in the 1930s (map created using Matlab R2012b).

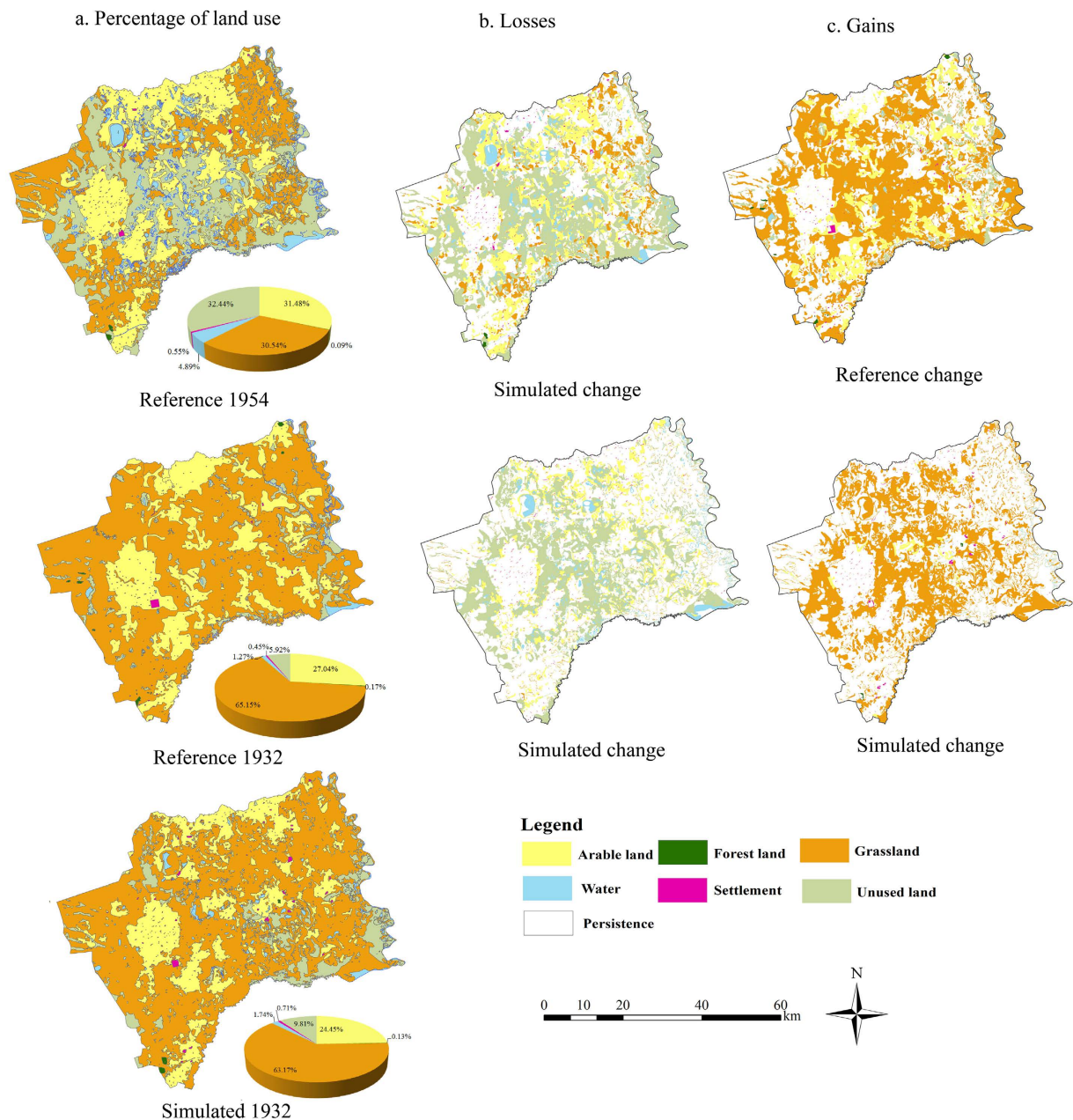


Figure 10. Percentage of each land-use category at three time points and the changes at two time intervals in the study area (map created using ARCGIS 10).

null model of no change. The HOC, MOC and FOC ratios were 0.532, 0.468 and 0.103, respectively. The figure of merit (FOM) was 48.19%, which is higher than in some previous case studies^{48,52,53}.

The analysis illustrated that the major differences among the three maps are less concerned with the simulation model; rather, they are related to the discrepancies in land category delineation between 1954 and 1932. The applications with a large FOM are those using the correct, or near-correct, net quantities for the categories in the prediction map. The large number of hits in the HLURM model might be explained by the fact that different definitions exist between the reference map of 1932 and the simulated map of 1932. It is possible that any precise measurement of simulation accuracy is unattainable due to time point inconsistencies concerning the definitions of land use categories. The majority of the topographic maps used in this study were produced between 1932 and 1935 for the Japanese military, while some were produced during the Manchukuo era for the Chinese military. Thus, these maps are limited primarily by the fact that they were created with a specific military purpose in mind. The maps also define certain types of land cover, such as arable land, settlements and water, however, other land-use types, such as unused land, are not clearly reflected. The land cover classes in each map are indicated based on their purpose and criteria. Accordingly, the grassland and unused land types drawn in the 1930s topographic maps are distinct from those derived from remote sensing images as a result of their different

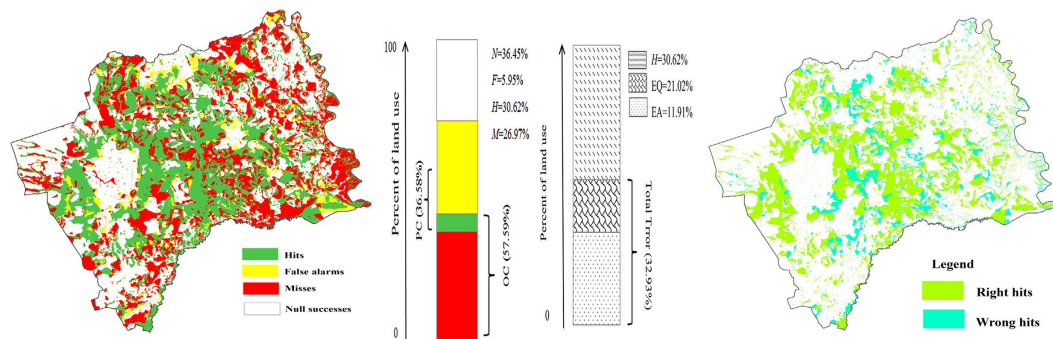


Figure 11. Prediction accuracy and error based on the 1954 (reference), 1932 (reference) and 1932 (simulated) land-use maps (map created using ARCGIS 10).

		Final Year (1932)						Initial total	Gross loss
		Arable land	Forest	Grassland	Water	Settlement	Unused land		
Initial Year (1954)	Arable land	<i>85202.00</i>	122.19	76904.66	461.23	1026.98	3638.65	167355.71	82153.71
		120681.57	70.78	44457.28	189.99	1547.65	408.45	167355.71	46674.14
	Forest	143.27	<i>76.74</i>	252.40	0.00	16.24	0.00	488.65	411.91
		2.59	467.59	10.73	0.00	2.76	4.98	488.65	21.06
	Grassland	24937.32	534.41	<i>123704.28</i>	1234.24	334.95	11626.66	162371.86	38667.58
		1983.44	106.57	157748.21	39.20	423.65	2070.79	162371.86	4623.64
	Water	3788.96	0.00	16556.56	<i>2797.54</i>	64.72	2792.23	26000.01	23202.47
		205.99	0.00	16743.07	7517.72	3.78	1529.45	26000.01	18482.29
	Settlement	1422.64	0.00	1192.72	2.93	<i>275.85</i>	50.44	2944.58	2668.73
		791.49	0.00	555.64	0.00	1584.42	13.04	2944.58	1360.16
Un used land	28250.58	148.62	127728.90	2263.89	664.62	<i>13388.77</i>	172445.37	159056.60	
	6301.00	30.76	116283.86	1527.24	196.31	48106.16	172445.33	124339.17	
	143744.76	881.97	346339.52	6759.83	2383.36	31496.74	531606.14	306161.00	
Initial total	129966.07	675.69	335798.79	9274.14	3758.57	52132.87	531606.14	195500.47	
Gross Gain	58542.77	805.23	222635.24	3962.29	2107.51	18107.97	306161.00		
	9284.50	208.10	178050.58	1756.42	2174.15	4026.71	195500.47		

Table 3. Area counts (ha) of persistence on the main diagonal (underlined) and change from the main diagonal between 1954 and 1932: reference change (in italics) and simulated change (in bold).

intended uses. For example, grassland is often combined with other land covers in the topographic maps, and thus its boundary is not easily determined. In addition, a large proportion of the grassland in these maps was categorized as wildland, resulting in limited areas of grassland being depicted on the maps. Rainfed lands and blank areas lacking a symbol are often difficult to decipher from grassland and wildland, making it challenging to extract and digitize grassland data. In the context of modern cartographic conventions, unused land is generally under-represented on historical maps. Thus, historical maps possess numerous limitations that must be considered in order to accurately interpret changes in land use. It is also necessary to recognize that discrepancies exist between the topographic maps and remote sensing images in respect to the information depicted. For instance, the period from 1900–1935 has been demonstrated to be a dry period in the history of northeastern China^{53,59}, confirming that the small area of wetland observed in the maps is an accurate reflection of the land cover of the time. Furthermore, considering the heterogeneity of the data sources, a combination of multi-source data should be used for future research. Blending multi-source data is conducive to extrapolating changes in the environment across a broad range of temporal and spatial scales, resulting in a more reliable representation of land use and land cover change. In comparison with our previous research where a cellular automata Markov model was used to reconstruct the spatial land use patterns in this study area⁴⁸, the HLURM model has performed better due to its consideration of more comprehensive land change driving factors. In this investigation we considered the effects of climate change on land use/cover, and the simulation results were more consistent with historical records. However, artificial adjustment in the quantity control module was only undertaken by considering the climate change drivers in this study. How to incorporate climate data into the simulated model is an area that requires further investigation.

Conclusions

Historical land use information is essential in understanding how anthropogenic land use and land cover change has influenced the temporal dynamics of environmental and ecological issues. To satisfy the growing demand

for harmonized, spatially explicit and high resolution land use change products, a spatial-explicit modeling framework (HLURM: Historical Land Use Reconstruction Model) was explored and proposed in this research to enhance our understanding of the degree and extent of global and regional anthropogenic changes in land use patterns. And then this modeling framework was applied to the historical reconstruction of spatial distribution of land use/cover in the early reclaimed time (1930 s) of Zhenlai County, northeastern China to check its modeling behavior. This was achieved by building a HLURM backward projection model in 90 m × 90 m spatial resolution based on three assumptions: that presently established spatial patterns of land use are intrinsically dependent on the historical patterns; that the boundary of historical land use with human activities does not exceed the union range of each land use type; and that factors relating to land suitability do not change over time. A three-map comparison methodology was then used to validate the projected reconstruction. The main conclusions are:

1. The HLURM model, consisting of four main modules (quantity control, spatial conversion rule, probability and spatial allocation), had a good performance in the spatial reconstruction of various land cover types. A CA model was also used to produce a backward simulation as a carrier.
2. The results of the historical reconstruction revealed that the largest percentage of the study area was grassland, followed by arable land and wetland. The remaining land-use categories comprised relatively smaller areas. Most of the arable land was located in the flat regions in the central and western areas, as well as in the north of the study area. Wetland areas were mainly distributed to the east and south along the Nenjiang and Taoer Rivers.
3. The total area change in the reference change map between 1954 and 1932 was 306,161.00 ha, while it was 195,500.47 ha for the simulated change map. Gross losses and gains in land-use categories were primarily concentrated in the central areas as well as those areas in the vicinity of rivers and lakes. The expansion of arable land at the expense of grassland was most probably due to the fast population growth experienced over the last few decades. The relative proportion of water bodies increased marginally as a result of increased precipitation. Between 1932 and 1954, a large proportion of grassland was transformed into unused land in both the change maps, especially in the reference change map, indicating that substantial environmental degradation had occurred.
4. The figure of merit of the model was 48.19%, which is higher than that estimated in several other case studies. Error due to allocation was 11.91%, while error due to quantity was 21.01%; this is likely as a result of the inconsistencies concerning category definitions between the maps. The major differences observed among the three maps are less concerned with the simulation model, but are more associated with the inconsistencies regarding how the land-use categories were defined during the study period, especially with regards to grassland and unused land types. For instance, in the topographic maps, grassland is often combined with other land covers, making its boundaries difficult to determine. Furthermore, a substantial portion of grasslands on the maps were often categorized as wildlands, resulted in difficulty extracting and digitizing the spatial extent of the grassland data. Therefore, it is crucial to select a reference map that has achieved high accuracy in the model validation for use in the three-map comparison. Unfortunately, due to the limited availability of historical data, it is often challenging to obtain a suitable reference map to be used to validate a reconstruction model.

References

1. Lambin, E. F. Modelling and monitoring land-cover change processes in tropical regions. *Progress in Physical Geography*, **21**, 375–393 (1997).
2. Turner, B. L., Lambin, E. F. & Reenberg, A. The emergence of land change science for global environmental change and sustainability. *Proceedings of the National Academy of Sciences* **104**, 20666–20671 (2007).
3. Foster, D. R. *et al.* The importance of land-use legacies to ecology and conservation. *Bioscience* **53**, 77–88 (2003).
4. Gragson, T. L. & Bolstad, P. V. Land use legacies and the future of southern Appalachia. *Society and Natural Resources* **19**, 175–190 (2006).
5. Fuchs, R. *et al.* A high-resolution and harmonized model approach for reconstructing and analyzing historic land changes in Europe. *Biogeosciences Discussions* **9** (2012).
6. Dupouey, J. L. *et al.* Irreversible impact of past land use on forest soils and biodiversity. *Ecology* **83**, 2978–2984 (2002).
7. Bakker, M. M. *et al.* Soil erosion as a driver of land-use change. *Agriculture, Ecosystems and Environment* **105**, 467–481 (2005).
8. Bolstad, P. V. & Swank, W. T. Cumulative impacts of land use on water quality in a southern Appalachian watershed. *Journal of the American Water Resources Association* **33**, 519–533 (1997).
9. Wear, D. N. & Bolstad, P. V. Land-use changes in Southern Appalachian landscapes: Spatial analysis and forecast evaluation. *Ecosystems* **1**, 575–594 (1998).
10. Pearson, S. G., Turner, M. G. & Drake, J. B. Landscape change and habitat availability in the southern: Appalachian highlands and Olympic peninsula. *Ecological Applications* **9**, 1288–1304 (1999).
11. Huston, M. A. The three phases of land-use change: implications for biodiversity. *Ecological Applications* **15**, 1864–1878 (2005).
12. Ellis, E. C., Antill, E. C. & Kreft, H. All is not loss: plant biodiversity in the anthropocene. *PLoS ONE* **7**, 1–9 (2012).
13. DeFries, R. S., Townshend, J. R. & Los, S. O. Scaling land cover heterogeneity for global atmosphere-biosphere models. *Scale in Remote Sensing and GIS* 231–246 (1997).
14. Brovkin, V. *et al.* Effect of anthropogenic land-use and land cover changes on climate and land carbon storage in CMIP5 projections for the 21st century. *Journal of Climate* **26**, 6859–6881 (2013).
15. Zaehle, S. *et al.* Projected changes in terrestrial carbon storage in Europe under climate and land-use change, 1990–2100. *Ecosystems* **10**, 380–401 (2013).
16. Houghton, R. A. Revised estimates of the annual net flux of carbon to the atmosphere from changes in land use and land management 1850–2000. *Tellus B*. **55**, 378–390 (2003).
17. Goldewijk, K. K. & Ramankutty, N. Land cover change over the last three centuries due to human activities: The availability of new global data sets. *GeoJournal* **61**, 335–344 (2004).
18. Ramankutty, N. & Foley, J. A. Estimating historical changes in global land cover: Croplands from 1700 to 1992. *Global biogeochemical cycles*, **13**, 997–1027 (1999).

19. Pongratz, J. *et al.* A reconstruction of global agricultural areas and land cover for the last millennium. *Global Biogeochemical Cycles* **22**, 1–16 (2008).
20. Hurtt, G. C. *et al.* China's land cover and land use change from 1700 to 2005: Estimations from high-resolution satellite data and historical archives. *Global Biogeochemical Cycles* **24**, 1–18 (2010).
21. Ye, Y. *et al.* Reconstruction of cropland cover changes in the Shandong Province over the past 300 years. *Scientific reports* **5**, 1–13 (2015).
22. Ye, Y. & Fang, X. Q. Spatial pattern of land cover changes across northeast China over the past 300 years. *Journal of Historical Geography* **3**, 408–417 (2011).
23. Pontius, R. G. Jr., Cornwell, J. D. & Hall, C. A. S. Modeling the spatial pattern of land-use change with GEOMOD2: Application and validation for Costa Rica. *Agriculture, Ecosystems & Environment* **85**, 191–203 (2001).
24. Bolliger, J. *et al.* Assessing ecological restoration potentials of Wisconsin (USA) using historical landscape reconstructions. *Restoration Ecology* **12**, 124–142 (2004).
25. Wulf, M., Sommer, M. & Schmidt, R. Forest cover changes in the Prignitz region (NE Germany) between 1790 and 1960 in relation to soils and other driving forces. *Landscape Ecology* **25**, 299–313 (2010).
26. Skaloš, J. *et al.* Using old military survey maps and orthophotograph maps to analyse long-term land cover changes—Case study (Czech Republic). *Applied Geography* **31**, 426–438 (2011).
27. Bender, O. *et al.* Using GIS to analyse long-term cultural landscape change in Southern Germany. *Landscape and urban planning* **70**, 111–125 (2005).
28. Boucher, Y. *et al.* Logging pattern and landscape changes over the last century at the boreal and deciduous forest transition in Eastern Canada. *Landscape Ecology* **24**, 171–184 (2009).
29. Hamre, L. N. *et al.* Land-cover and structural changes in a western Norwegian cultural landscape since 1865, based on an old cadastral map and a field survey. *Landscape Ecology* **22**, 1563–1574 (2007).
30. He, F., Li, S. & Zhang, X. A spatially explicit reconstruction of forest cover in China over 1700–2000. *Global and Planetary Change* **131**, 73–81 (2015).
31. Yang, X. *et al.* Research on reconstructing spatial distribution of historical cropland over 300 years in traditional cultivated regions of China. *Global and Planetary Change* **128**, 90–102 (2015).
32. Kumar, S. *et al.* Characterizing long-term land use/cover change in the United States from 1850 to 2000 using a nonlinear bi-analytical model. *AMBIO* **42**, 285–297 (2013).
33. Yang, Y. Y. *et al.* A review of historical reconstruction methods of land use/land cover. *Journal of Geographical Sciences* **24**, 746–766 (2014).
34. Zhu, F., Cui, X. F. & Miao, L. J. China's spatially-explicit historical land-use data and its reconstruction methodology. *Progress in Geography* **31**, 1563–1573 (in Chinese) (2012).
35. Goldewijk, K. K. *et al.* The HYDE 3.1 spatially explicit database of human-induced global land-use change over the past 12,000 years. *Global Ecology and Biogeography* **20**, 73–86 (2011).
36. Ciais, P. *et al.* Effects of land use change and management on the European cropland carbon balance. *Global Change Biology* **17**, 320–338 (2011).
37. Schulze, E. D. *et al.* The European carbon balance. Part 4: integration of carbon and other trace-gas fluxes. *Global Change Biology* **16**, 1451–1469 (2010).
38. Miao, L. J. *et al.* China's land-use changes during the past 300 years: a historical perspective. *International Journal of Environmental Research and Public Health* **13**(9), 847 (2016).
39. Cui, X. F. *et al.* Land-Use Changes in China: Historical Reconstruction Over the Past 300 Years and Future Projection. *World Scientific* (2015).
40. Cao, X. Reconstruction and change analysis of cropland data of China in recent 300 years. *Acta Geographica Sinica* **69**(7), 896–906 (in Chinese) (2014).
41. Lv, Y. The spatial reconstruction of land use/land cover in the early reclaimed time of the western Jilin Province. *Changchun: Jilin University* (in Chinese) (2012).
42. Lv, Y., Zhang, S. W. & Yang, J. C. Application of toponymy to the historical LUCC researches in Northeast China: Taking Zhenlai county of Jilin province as an example. *Journal of Geo-Information Science* **12**(2), 174–179 (in Chinese) (2010).
43. Lv, Y., Zhang, S. W. & Yang, J. C. Reconstruct the spatial distribution of land use/land cover in the early reclaimed time of the western Jilin Province—Based on the GEOMOD model. *Journal of Anhui Agricultural Sciences* **43**(13), 304–308 (in Chinese) (2015).
44. Bai, S. Y. & Zhang, S. W. The discussion of the method of land utilization spatial information reappearance of history period. *J. Arid Land Resour. Environ* **18**, 77–80 (In Chinese) (2004).
45. Bai, S. Y., Zhang, S. W. & Zhang, Y. Z. Study on the method of diagnose the plow land spatial distribution in historical era. *Syst. Sci. Compr. Stud. Agric.* **21**, 252–255 (In Chinese) (2005).
46. Liu, J. Y. *et al.* Study on spatial pattern of land-use change in China during 1995–2000. *Science in China Series D: Earth Sciences* **46**, 373–384 (2003).
47. Yang, Y. Y. *et al.* Spatiotemporal changes of farming-pastoral ecotone in Northern China, 1954–2005: A case study in Zhenlai County, Jilin Province. *Sustainability* **7**, 1–22 (2015a).
48. Yang, Y. Y. *et al.* Using a Cellular Automata-Markov Model to Reconstruct Spatial Land-Use Patterns in Zhenlai County, Northeast China. *Energies* **8**, 3882–3902 (2015b).
49. Chen, H. & Pontius, R. G. Jr. Diagnostic tools to evaluate a spatial land change projection along a gradient of an explanatory variable. *Landscape Ecology* **25**, 1319–1331 (2010).
50. Chen, H. & Pontius, R. G. Jr. Sensitivity of a land change model to pixel resolution and precision of the independent variable. *Environmental modeling & assessment* **16**, 37–52 (2011).
51. Santé, I. *et al.* Cellular automata models for the simulation of real-world urban processes: a review and analysis. *Landscape and Urban Planning* **96**, 108–122 (2010).
52. Pontius, R. G. Jr. *et al.* Comparing the input, output, and validation maps for several models of land change. *The Annals of Regional Science* **42**, 11–37 (2008).
53. Gao, P. *et al.* Trend Analysis of Precipitation in Northeast China in Recent 100 Years. *Journal of China Hydrology* **30**, 80–84 (in Chinese, English summary) (2010).
54. Samat, N., Hasni, R. & Elhadary, Y. A. E. Modelling land use changes at the peri-urban areas using geographic information systems and cellular automata model. *Journal of Sustainable Development* **4**, 72–84 (2011).
55. Lin, N. F. *et al.* Constructions of a geo-information atlas-spatial analysis model toward a perspective of the spatial pattern changes in land use. *Quaternary Sciences* **29**, 711–723 (in Chinese, English summary) (2009).
56. Gimmi, U., Bürgi, M. & Stuber, M. Reconstructing anthropogenic disturbance regimes in forest ecosystems: A case study from the Swiss Rhone valley. *Ecosystems* **11**, 113–124 (2008).
57. Wang, Z. M. *et al.* Extracting land use information based on topographical map and knowledge rules. *Geo-inf. Sci.* **10**, 67–73 (In Chinese) (2008).
58. Poska, A. *et al.* Using quantitative pollen-based land-cover estimations and a spatial CA_Markov model to reconstruct the development of cultural landscape at Rõuge, South Estonia. *Vegetation History and Archaeobotany* **17**, 527–541 (2008).
59. Sun, F. H., Yuan, J. & Lu, S. The change and test of climate in Northeast China over the last 100 years. *Climatic and Environmental Research* **11**, 101–108 (in Chinese) (2006).

Acknowledgements

This research was funded by the grants from National Youth Science Foundations (No. 41601173; No. 41301467) and China Postdoctoral Science Foundation (No. 2016M600954).

Author Contributions

Y.Y. wrote the main manuscript; S.Z. collected and prepared the data; Y.L. and X.X. provided technical guidance; A.S. edited the manuscript and provided valuable suggestions. All authors accepted the final version of the manuscript.

Additional Information

Competing financial interests: The authors declare no competing financial interests.

How to cite this article: Yang, Y. *et al.* Analyzing historical land use changes using a Historical Land Use Reconstruction Model: a case study in Zhenlai County, northeastern China. *Sci. Rep.* 7, 41275; doi: 10.1038/srep41275 (2017).

Publisher's note: Springer Nature remains neutral with regard to jurisdictional claims in published maps and institutional affiliations.



This work is licensed under a Creative Commons Attribution 4.0 International License. The images or other third party material in this article are included in the article's Creative Commons license, unless indicated otherwise in the credit line; if the material is not included under the Creative Commons license, users will need to obtain permission from the license holder to reproduce the material. To view a copy of this license, visit <http://creativecommons.org/licenses/by/4.0/>

© The Author(s) 2017